STUDY OF GRAPHENE OXIDE-POLYMER NANOCOMPOSITE (GPN) ADSORPTIVE MEMBRANE FOR LEAD REMOVAL FROM WASTEWATER

NIK-RASHIDA NIK-ABDUL-GHANI[1],
MOHAMMED SAEDI JAMI[1,*], NURUL-SAKINAH ENGLIMAN[1],
MUTIU KOLADE AMOSA[2], MOHAMED HASNAIN ISA[3]

[1]Department of Biotechnology Engineering, Faculty of Engineering, International Islamic University Malaysia, Jalan Gombak, 53100 Kuala Lumpur, Malaysia
[2]Waste Management Unit, HSE Division, Department of Petroleum Resources, 7 Kofo Abayomi Street, Victoria Island, Lagos 101241, Nigeria
[3]Civil Engineering Programme, Universiti Teknologi Brunei, Tungku Highway, Gadong BE1410, Brunei Darussalam
*Corresponding author: saedi@iium.edu.my

Abstract

The utilisation of polymeric membrane has been reported in numerous investigations on wastewater management of heavy metals. In this work, graphene oxide-polymer nanocomposite (GPN) adsorptive membranes were fabricated via non-solvent induced phase inversion (NIPS) method for lead removal. The modification of polyethersulfone (PES) membrane was conducted by incorporating graphene oxide (GO) in the matrix polymer solution. The characterisation of the GPN membranes were investigated through porosity, scanning electron microscopy (SEM) and atomic force microscopy (AFM). Optimisation of batch adsorption experiments on the GPN membrane fabricated with 0.5 wt.% of GO with the addition of 0.5 wt.% of polyvinylpyrrolidone (PVP) exhibited the highest lead removal that is about 97.81% under 60 minutes exposure and acidic condition (pH 5). Langmuir isotherm model was found to be the best-fitting for the lead adsorption process. The findings indicated that the monolayer adsorption mechanism occurred on the surface of the GPN membrane.

Keywords: Graphene oxide, Lead removal, Nanocomposite adsorptive membrane, Optimisation adsorption, Wastewater treatment.

1. Introduction

Heavy metals contamination in water or wastewater is of global concern. This water pollution has set imbalanced global water appropriation and has adversely tilted towards the declining line of freshwater availability. In order to meet the increasing demand of clean and quality water for drinking and daily usage, many approaches have been developed in water and wastewater treatment. Lead is one of the common and most toxic pollutants in natural waters. Lead contaminations present in water sources are usually associated with mining industries such as petroleum mining, smelting, lead-acid battery manufacturing and incineration of solid wastes [1-3]. According to Malaysia Environmental Quality Report [4], lead is one of the highest contaminants' concentration found in tested water and it falls under Class II risk. Lead pollutants pose serious health issues towards human and ecosystem.

The reuse of treated wastewater is a key access to discover new water resources. Development of membrane technology plays a significant role in water/wastewater treatment due to its simplicity in operation, cost effectiveness, high productivity, high removal capacity and scale-up easiness [5]. Recently, nanomaterials have been added in membrane fabrication to improve the properties, reduce biofouling, reduce fabrication and maintenance cost and higher efficiencies [6-9]. The integration of membrane technology and nanotechnology has further increased the effectiveness of adsorbent materials providing innovative systems to novel adsorptive membranes for improving wastewater treatment. Notably, carbon-based nanomaterials such as carbon nanotubes, graphene and its derivatives have shown high ability in adsorptive membrane due to high mechanical strength, high resistance to acids/alkaline or inorganic solvents and convenience to use [10-12]. The specific functional groups and the exclusive structural properties of the adsorptive membrane are key factors in supporting the adsorption removal of heavy metal ions from wastewater [13]. Moreover, this adsorptive membrane which has a dual function of adsorption and filtration owns its unique characteristics such as low energy consumption, high porosity, high desorption efficiency and ease of fabrication [5].

One of the promising materials is graphene oxide (GO), the nanoparticle with unique two-dimensional, single atomic thick structure, high specific surface area and high surface activity properties [14-17]. GO also becomes the forefront research in membrane fabrication for wastewater treatment due to its strong mechanical stability, hydrophilicity, high negative charge density, ease of fabrication, chemical inertness, industrial scale production and the ability to adsorb heavy metals from wastewater [18, 19] The fabrication of free-standing GO membrane is widely utilized as separation layer in many applications such as molecular and ion separation [15], oil/water separation [20], dehydration of ethanol [21] and ion dialysis separation [22]. These studies showed that the efficient separation performance have been achieved using this free-standing GO membrane due to its high hydrophilicity and structural stability strength [12]. However, the free-standing GO membrane is relatively flat with a thickness less than 100 nm, thus it is difficult to measure the area and to use it without any support material [23]. Its poor permeability and low anti-pressure ability also limit its utilisation in high-pressure applications [17]. Therefore, slight modification of the GO membrane by incorporating it with polymeric substance can improve the separation performance and hydrophilicity of the membranes for wider separation applications [12, 24, 25].

Modification of membrane will increase the membrane adsorption in the separation process. One of the approaches to increase the membrane adsorption is fabrication of asymmetric membrane with a thin, dense layer on top region supported by a porous substructure layer with high mechanical strength [26-28]. Moreover, limited information on the interaction between membrane adsorbent and adsorbate remains a great challenge to the knowledge of adsorption mechanism [29]. Thus, adsorption isotherm study can be utilized to explain in detail the mechanism of lead ions on to the modified GO adsorptive membrane that has been influenced by parametric effects such as pH, initial concentration and contact time [30]. Moreover, fabrication of asymmetric membrane by non-solvent induced phase separation (NIPS) method offers improved adsorptive membrane separation performance due to high permeability of support layer. It is rarely gets blocked hence its intensive usage in ultrafiltration, nanofiltration and reverse osmosis membrane [26, 31, 32].

Therefore, the aim of this study is to fabricate the asymmetric GO nanocomposite membrane via NIPS method for lead removal. The modification of polyethersulfone (PES) membrane was conducted by incorporating graphene oxide GO in the matrix polymer solution. This was done by varying several parameters such as concentrations of GO, addition of pore former i.e. polyvinylpyrrolidone (PVP) during the polymer dissolution and membrane casting. The adsorption optimisation for each of fabricated graphene oxide polymer nanocomposite (GPN) membrane was investigated with various parametric conditions including pH, initial concentration and contact time. The best fabricated GPN adsorptive membrane was tested for the adsorption study via batch process. Then, the desorption and regeneration study of the membrane were conducted to evaluate the quality of the GPN adsorptive membrane for practical use. Synthetic wastewater containing lead solution was used as a source of tested wastewater.

2. Materials and Method

All reagents used for fabrication were analytical grade. Graphite powder (particle size < 50 µm) was supplied by R&M Chemicals, Canada. Lead nitrate (PbNO$_3$; 99%) was purchased from R&M Chemicals. Deionized water was used as the nonsolvent for polymer precipitation and for samples preparation. Commercial grade polyethersulfone (PES) (Ultrason E6020P, MW = 75,000 g/mol and glass transition temperature 225 °C) was supplied by BASF, Ludwigshafen, Germany. Polyvinylpyrrolidone (PVP) (MW = 40,000 g/mol) was used as pore forming additive for the membrane preparation and N, N- dimethylformamide (DMF, 99.5%) as solvent, and were all purchased from R&M Chemicals, Canada. The process optimisation and statistical analysis were designed and performed using Design Expert® software version 12 (STAT-EASE Inc., Minneapolis, USA).

2.1. Synthesis of graphene oxide and fabrication of membrane

GO were synthesized according to Hummer's method with some modifications [39]. The produced GO was then utilized for membrane fabrication. The GPN membranes were fabricated by the NIPS method according to Wang et al. [33] with some modifications. N, N- dimethylformamide (DMF) was used as a solvent and deionized water as the non-solvent. The composition of each casting solutions was prepared according to the different percentages of the GO and PVP relative to the polymer matrix weight as outlined in Table 1 [34]. Firstly, GO were dispersed in DMF and

sonicated for 1 h. Then, PES and PVP were added in the above mixture and was stirred at 50 °C for 24 h to obtain a well-dispersed casting solution. Then, the resulting homogenous casting solution was put on ultrasonic bath and degassed to eliminate air bubbles. Subsequently, the casting solution was poured on a clean glass plate (210 × 297× 5 mm) to cast the membrane of 300 μm thickness. After 60 seconds of pre-evaporation at room temperature (28± 2° C), it was immersed into the non-solvent bath (coagulation bath) and kept in the container up to 24 h. The prepared membrane was washed with deionized water and then preserved in water before use.

Table 1. Composition used for GPN membrane fabrication.

GPN membrane	PES (wt.%)	DMF (wt.%)	GO (wt.%)	PVP (wt.%)
GPN0	17.0	83.0	-	-
GPN1	17.0	82.9	0.1	-
GPN2	17.0	82.5	0.5	-
GPN3	17.0	82.0	1.0	-
GPN4	17.0	82.0	0.5	0.5

Note: GPN0: bare PES membrane; GPN1: 0.1 wt.% GO; GPN2: 0.5 wt.% GO; GPN3: 1.0 wt.% GO; GPN4: 0.5 wt.% GO and 0.5 wt.% PVP.

2.2. Characterisation of PES-GO membrane

Characterisation of the fabricated GPN membrane was achieved by conducting membrane porosity test, SEM and AFM analysis. The porosity of membranes was determined by gravimetric method as described elsewhere [35]. Firstly, dried membranes were cut out with 1.5 cm × 1.5 cm dimension. Then the squared membranes were immersed in the deionized water for 24 h at room temperature (28± 2° C) to allow water penetration into the membrane pores. Subsequently, the water on the membrane surface was dried by tissue paper and then the membranes were weighed using analytical balance (B204-S, Mettler Toledo, Switzerland) to estimate the quantity of water adsorbed in the pores. Finally, the membrane was weighed again after the remaining water inside the membranes was vacuum dried in a vacuum oven (LV02030, LabTech, Daihan) at 60 °C for 6 h. The porosity, ε was determined using Eq. (1) [35].

$$\varepsilon = \frac{\frac{W_w - W_d}{\rho_w}}{\left(\frac{W_w - W_d}{\rho_w} + \frac{W_d}{\rho_p}\right)} \times 100 \tag{1}$$

where w_w and w_d correspond to the weight of wet membrane and the weight of dried membrane, respectively. Meanwhile, ρ_w is the water density (0.998 g/cm^3) and ρ_p is the PES density (1.37 g/cm^3) at the room temperature (28± 2° C).

The roughness and topography of the membrane was determined by tapping mode of atomic force microscopy, AFM (Tosca 400, Anton-Paar GmbH, Austria). The surface and cross-section morphology of the GPN membranes were observed by SEM (JSM-IT 100, Jeol, Japan) after coating with a thin gold film using sputter coater device (Q-SC7620, Quorum Tech Ltd., London).

2.3. Batch adsorption experiment

The optimisation of batch adsorption experiments was designed by 2-level factorial and conducted with four centre points and 3FI model. The number of runs for the adsorption optimisation for membrane as unveiled by the DOE statistical software

were 12 runs. All the experiments were replicated and their concentrations were measured. Throughout the optimisation study, independent variables for pH, initial concentration and contact time were represented as variable *A*, *B* and *C*, respectively. The variables range and levels examined in this study are shown in Table 2.

Table 2. Range and levels of categorical factors by DOE.

Factor	Name	Units	Type	Low Actual	High Actual	Low Coded	High Coded
A	pH		Numeric	5	9	-1	1
B	Initial concentration	ppm	Numeric	100	500	-1	1
C	Contact time	min	Numeric	10	60	-1	1

Batch adsorption experiments were done to determine the quantitative uptake of lead by the GPN membrane. The effect of different variables/factors on adsorption process were investigated including concentration, contact time, and pH [36]. Synthetic wastewater containing lead were prepared using lead nitrate stock solution, with varying initial concentrations of 100 ppm, 300 ppm and 500 ppm. The experiments for batch adsorption were done in a 100 mL conical flask. The membrane was cut into small pieces (total weight of 1 ± 0.0048 g) with 1.5×1.5 cm squares. The weight of membrane was obtained as a wet weight where the membrane was cleaned and dried with a filter paper before weighing process. The pH value was adjusted using either 1M of NaOH or 1M of HCl until the required pH values of 5, 7 or 9 was attained. Then, the membrane was added to each of the flasks containing the 100 mL of synthetic lead-contaminated wastewater and the mixture was mixed/agitated continuously using laboratory shaker with constant speed of 200 rpm. After a pre-determined contact time set at 10, 35 or 60 min, the treated samples were extracted, and the absorbance was measured using UV-Vis spectrophotometer immediately. The removal efficiency was calculated according to Eq. (2) [37, 38]:

$$\% \, removal = \frac{c_o - c_t}{c_o} \times 100 \tag{2}$$

where C_o and C_t are the initial and final concentrations of lead in the solution (ppm), respectively.

2.4. Adsorption isotherm

Adsorption isotherm analysis was conducted to determine the equilibrium point of lead adsorption on the GPN4 membrane. Six different initial lead concentrations were prepared (100, 200, 300, 400, 500 and 600 ppm) and the GPN4 membrane (1 ± 0.0048 g) was added to each of a 100 mL lead solution in a conical flask. The batch experiment has proceeded at optimum parametric conditions of highest lead removal efficiency which are at constant pH (pH 5) and contact time (10 minutes) and continuously agitated at 200 rpm. After pre-determined time, the treated samples were extracted, and the absorbance were measured using spectrophotometer to analyse the residual concentration of lead.

Two common isotherm models, Langmuir and Freundlich models were utilised to determine the adsorption equilibrium. The Langmuir isotherm model indicates that the adsorption of heavy metals occurs by monolayer adsorption on a homogeneous surface where the adsorption sites have equal affinities toward the adsorbate.

Meanwhile, the Freundlich isotherm model describes that the uptake of metal ions occurs on a heterogeneous surface without uniform distribution of adsorption heat on the surface [39]. The Langmuir model is given as in Eq. (3)[25, 40] :

$$\frac{1}{q_e} = \left(\frac{1}{bq_m}\right)\frac{1}{C_e} + \frac{1}{q_m} \tag{3}$$

where, q_e is the quantity of adsorbate adsorbed in mg/g, C_e is the equilibrium concentration (mg/L), b is the constant of adsorption equilibrium (L/mg) and q_m (mg/g) is the maximum adsorption capacity. Meanwhile, the Freundlich isotherm model in a linear form expression as shown in Eq. (4)[40, 41]:

$$\log q_e = \log K_f + \frac{1}{n}\log C_e \tag{4}$$

where K_f is an indicator of adsorption capacity while *1/n* is a measure of intensity of adsorption. Adsorption equilibrium is determined from the uptake-time data. From both isotherm models, linear regression values (R^2) were calculated to describe the mechanism of adsorption process. The R^2 value which is approximately 1.00 indicates that the adsorption process conforms better to a specific isotherm model.

2.5. Determination of lead concentration by spectroscopy

Spectroscopy method to determine lead ion in aqueous solution is one of the non-destructive methods without addition of chemical reagent. To determine the standard curve and final concentration of lead, UV spectroscopy method is conducted according to Tan et al. [42] with slight modification. The samples were prepared from lead nitrate stock solution. For standard curve determination, a series of lead concentrations from 25 ppm to 250 ppm solutions were prepared, and then measured immediately with the aid of Secomam UviLine (Kisker, Steinfurt, Germany) spectrophotometer at 225 nm [42]. The final concentration of the lead is determined by interpolation on the standard curve graph.

2.6. Desorption and regeneration study

The reusability of GPN4 towards lead removal was investigated based on simple desorption and regeneration experiment using batch adsorption system according to Bayuo et al. [43] with slight modification. Succeeding to the completion of lead adsorption-desorption experiment, GPN4 saturated with lead ions was soaked in 0.1 M HCl solution (pH 3) for 1 h followed by washing for 2 consecutive times with deionized water. Batch adsorption study was then performed again to re-assess the membrane adsorption capability at same optimum conditions of pH 5, initial concentration of 100 ppm, contact time of 60 minutes and constant agitation of 200 rpm. The regenerated sample was collected, and the final concentration was measured using spectrophotometer.

3. Results and Discussion

3.1. Membrane porosity

The porosity of the membrane was obtained gravimetrically as described in Section 2.3. The percentage of porosity for each membrane were calculated and illustrated in the Fig. 1.
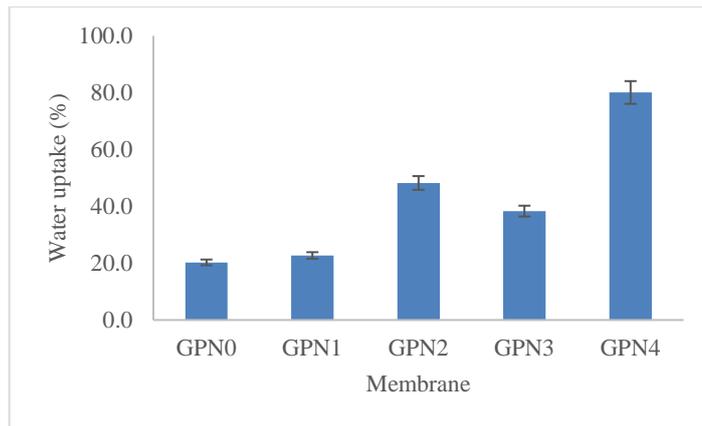
Fig. 1. Percentage of porosity for GPNs membrane.
GPN0: bare PES membrane; GPN1: 0.1 wt.% GO; GPN2: 0.5 wt.% GO;
GPN3: 1.0 wt.% GO; GPN4: 0.5 wt.% GO and 0.5 wt.% PVP.

The bare PES which is GPN0 showed the lowest porosity due to its hydrophobic nature of PES. Increasing the amount of GO from 0.1 wt.% to 0.5 wt.% led to the increase in porosity of membrane from 22.7% to 48.2% for GPN1 and GPN2, respectively. However, further increase in GO up to 1.0wt.% reduced the porosity of GPN3 which could be due to agglomeration of the GO during casting of the membranes. This phenomenon is similar with previous findings which reported that the agglomeration of GO occurred at higher concentration of nanoparticle loadings [44, 45]. This aggregation of the GO is because of the strong van der Waal interactions between particles and the functional groups [46, 47]. On the other hand, fabricated membranes with the addition of PVP (GPN4) displayed the highest percentage of water uptake indicating increase in porosity when the pore forming agent was added because of the hydrophilic nature of PVP which usually enhances the instantaneous de-mixing of the polymer, PVP and GO as previously reported [25, 36]. This result indicated that an increase in the amount of GO will lead to an increase in the viscosity of the solution which eventually results in low porosity of membrane thereby delaying the liquid-liquid exchanging process [48, 49]. Therefore, it is suggested that the optimum amount of GO of 0.5 wt.% where normally a small addition of GO (<1.0 wt.%) significantly improves polymeric membrane physicochemical properties as reported by Wang et al. [24].

3.2. SEM and AFM analysis

The characterisation of membrane on SEM and AFM analysis were reported on GPN4 adsorptive membrane only since it provides the highest water uptake among all membranes in this study, and for the conciseness of the report. The SEM images for surface and cross-section of asymmetric GPN4 membrane are shown in Fig. 2. As shown in this Fig. 2(a), the surface is relatively smooth, and the agglomeration or lump of GO is not seen in the surface. The carbon-based structure of GO and the interaction of GO makes it well dispersed in the polymer casting solution and no accumulation of GO was observed. The result indicated that good stability between GO, PES and PVP [35, 50]. Normally,

addition of additives and nanofiller would increase the pore size of the membrane. From the cross-section image of the membrane, it is revealed that the asymmetric structure of membrane composed of finger like shape due to addition of nanoparticle, GO and pore forming agent, PVP. This asymmetric nanopores structure observed on the GPN4 plays an important role for the lead adsorption. As observed, the addition of GO showed the wider finger-like channel of the membrane and increased the porosity of the membrane significantly [51]. The addition of PVP in the membrane enhances water diffusion rates between the solvent and the non-solvent during the phase inversion process in the coagulation bath and formed the finger-like voids as shown in the image [35].

(a)

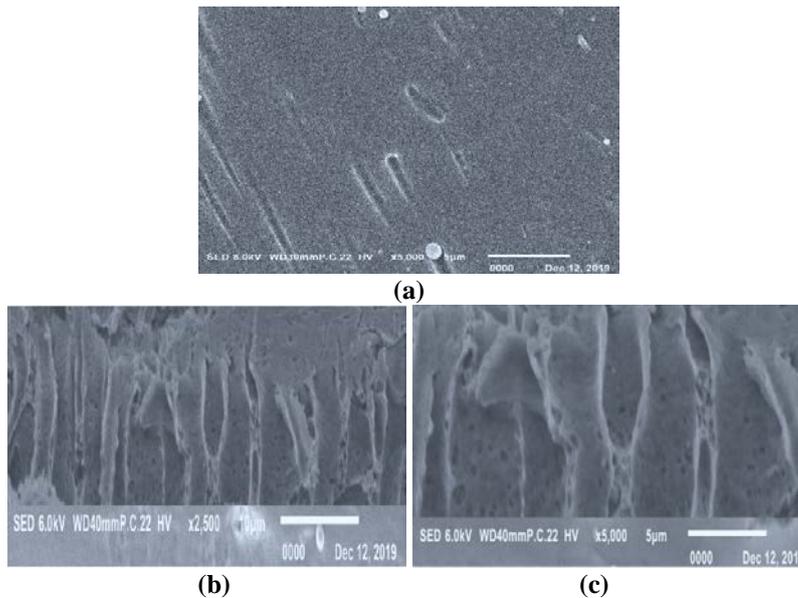
(b)   (c)

Fig. 2. (a) surface morphology of GPN4 with 5000× magnification and cross-section morphology of GPN4 with (b) 2500× magnification and (c) 5000× magnification.

The AFM analysis was reported on GPN4 membrane and its surface topography image is displayed in Fig. 3. The root-mean-square height (S_q) value obtained is 19 nm which indicates the surface roughness of the sample. This GPN membrane surface roughness value showed lower surface roughness compared with the previously reported neat PES membrane (S_q value range 26- 65 nm) [25, 52, 53]. The S_q value is decreased due to the diffusion of GO onto the surface of membrane and acceleration of phase exchange during the coagulation in phase inversion process [25, 52]. This result suggests that the roughness of the GPN4 membrane is smoother than neat PES indicating that nanofiller is well-incorporated in the polymer matrix as opined in previous study [53]. On the other hand, membrane with lower surface roughness value provides more robust antifouling.
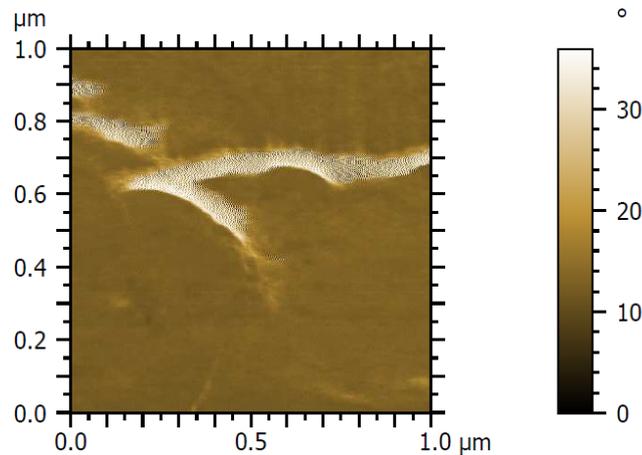
**Fig. 3. Surface topography of GPN4 from tapping
mode of AFM measurements under ambient conditions.**

3.3. Batch adsorption

The batch adsorption experiments were conducted utilising GPN4 in replicate. The results for percentage removal of lead were tabulated in Table 3. The value of absorbance from the spectrophotometer was measured three times and their average was calculated. After that, the percentage removal for each of the membrane was calculated and compared.

From Table 3, it can be deciphered that the GPN4 membrane has highest percentage removal (97.81%) at acidic condition (pH 5), initial concentration of 100 ppm and contact time of 60 minutes. The adsorption capacity of lead was found to be maximum in acidic condition (pH 5) and lower at pH 7 and pH 9. This situation could be best explained by the neutralisation of functional groups which must have contributed to the competition between proton and lead ions at lower pH [54]. As the initial lead concentration increased from 100 ppm to 500 ppm, the percentage lead removal decreased from 97.81 to 50.18%. This may be attributed to the fact that at low concentrations the ratio of surface-active sites to the total lead ions in the solution is high and hence all lead ions may interact with the membrane sites thus allowing the adsorption to take place [55]. The lead removal efficiency increased with the increase in contact time from 10 to 60 minutes and then remained constant. This result ascribed to the adsorption equilibrium of the membrane was achieved as previously reported by others [36, 56]. Moreover, the adsorption time is sufficiently long enough to overcome the diffusion limitation [13].

The mechanism of adsorption at solid-liquid interface of the GPN adsorptive membrane and the lead ions could be explained by electrostatic interactions. The carboxylic acid (-COOH) on the membrane surface may be ionized when in contact with the lead solution, carrying a negative or positive charge thus enabling the electrostatic force interactions [57]. In addition, the oxygen containing groups of the GPN adsorptive membrane and its hydrophilicity could make it easy to adsorb metal ions through interstitial diffusion [13].

Table 3. Lead removal efficiency
of batch adsorption for GPN4 membrane.

A: pH	B: Initial concentration (ppm)	C: contact time (min)	Removal efficiency (%)
7	300	35	92.84± 1.62
9	100	60	74.65± 1.97
5	500	10	52.83± 1.67
9	500	10	90.96± 0.36
5	**100**	**60**	**97.81± 0.36**
7	300	35	93.92± 0.15
9	500	60	95.54± 0.55
5	100	10	94.46± 0.26
5	500	60	50.18± 8.11
7	300	35	94.07± 0.15
7	300	35	90.46± 0.71
9	100	10	67.37± 2.12

Note : ± symbol showing the error of the repeating experiments in replicate.

3.4. Adsorption isotherm and regeneration studies

The adsorption isotherm was conducted on GPN4 membrane at the optimum operating conditions of pH 5 and contact time of 60 minutes at various initial lead concentrations in the range of 100-600 ppm. The adsorption mechanism was investigated using two isotherm models namely Langmuir and Freundlich to determine the adsorption equilibrium. The equilibrium plot was presented as Fig. 4, while the linearized graph of both Langmuir and Freundlich isotherms were plotted as shown in Figs. 5 (a) and (b), respectively. The calculated isotherm parameters were summarized in Table 4.
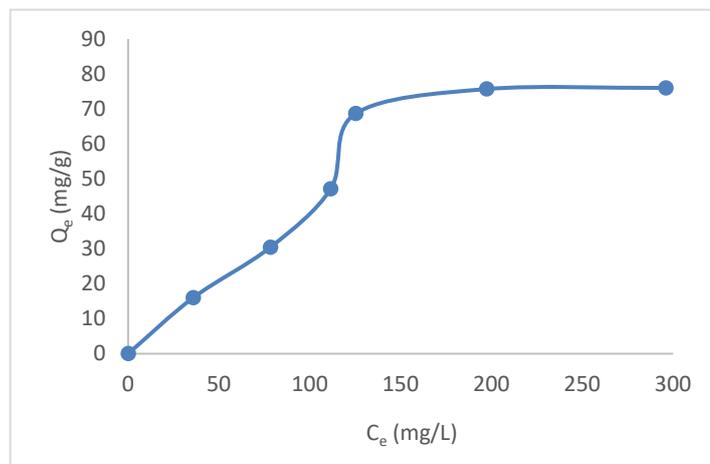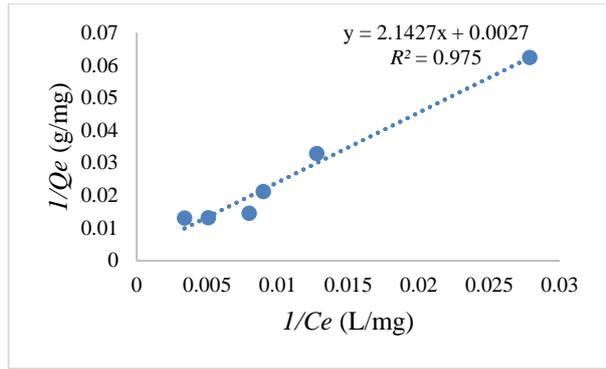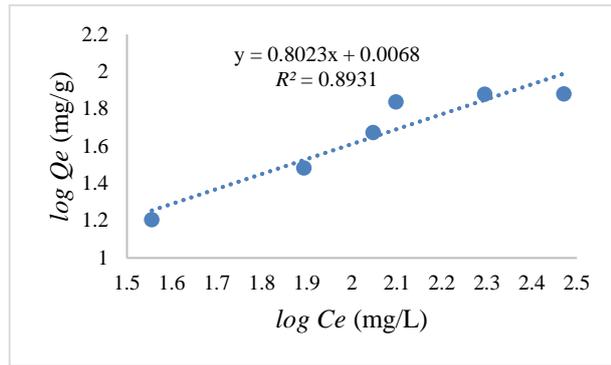

Fig. 4. Graph of equilibrium; concentration of lead on the surface
of GPN4, q_e, versus the concentration of the lead in the solution, C_e.

(a)

(b)

**Fig. 5. Linearized plot of (a) Langmuir
isotherm model and (b) Freundlich isotherm model.**

Table 4. Isotherm parameters for Langmuir and Freundlich models.

Isotherm model	Isotherm parameter		
Langmuir	Q_{max} (mg/g)	K_L (L/mg)	R^2
	370.37	0.00126	0.975
Freundlich	n	K_f (mg/g)	R^2
	1.2464	1.0157	0.8931

The favourable adsorption mechanism is dependent on the higher regression value (R^2) of close to a value of 1.0. Based on the outcomes, the R^2 value of 0.975 for Langmuir model was higher than the R^2 value of 0.893 for Freundlich model. Therefore, in this study, the Langmuir model offered the most appropriate model for fitting the adsorption of lead ions onto the GPN4 membrane by monolayer adsorption mechanism. Numerous reports have stated that modified PES membrane with graphene-based nanoparticles were fitted to Langmuir isotherm [38, 58, 59]; where the monolayer adsorption occurred at homogeneous surface of the membrane.

The saturated lead ions of GPN4 membrane was then subjected to simple desorption method (using acidic solution) to regenerate its adsorption ability for next cycle use. The resultant of three successive adsorption-desorption using 0.1 M HCl

as desorption agent can be observed in Fig. 6. This phenomenon ascribed that desorption using acidic solution might involving ion exchange type interaction [43].
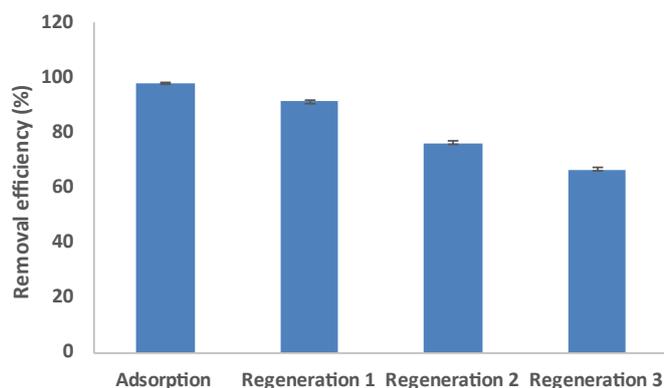

Fig. 6. Adsorption-desorption and regeneration study of GPN4 membrane.

The GPN4 is reported to exhibit 91% of removal efficiency after completing first regeneration process. For the subsequent second and third cycle of regeneration process, the recovery rate of the GPN4 gradually decreased from 76.2% to 66.5%, respectively. The findings confirm that after exposing to proper desorption process the GPN4 can be recycled for several times before its adsorption capability is reduced by half. This result is comparable with other GO nanocomposite membranes that reported the reusability up to third regeneration cycle for heavy metals removal [38, 60, 61].

4. Conclusions

In this study, GO was synthesized and incorporated into the PES for mixed matrix membrane fabrication via NIPS method. The addition of GO increased the hydrophilicity, porosity and adsorption capacity compared to the bare PES. Moreover, the membrane with the addition of pore forming agent (PVP) featured higher efficiency with highest percentage removal of lead (97.81 %) at optimum operating conditions of pH 5, 10 minutes of contact time and 100 ppm of initial lead concentration. The adsorption isotherm on the GPN4 was done and Langmuir isotherm model was found to be the most fitting. This is an indication that the monolayer adsorption mechanism of lead on the GPN4 membrane dominated. It is therefore believed that embedment of GO and PVP to modify the polymeric membrane is an excellent approach to develop antifouling membrane and increase the membrane mechanical properties better than neat PES membrane. Therefore, future research on utilisation of the GPN membrane using dynamic filtration will be needed to analyse the fouling phenomenon in such a way it can withstand repeated adsorption/desorption and filtration processes using a modular membrane system.

Acknowledgement

Nomenclatures

b	Constant of adsorption
C_e	Equilibrium concentration, mg/L
C_o	Initial concentration of lead
C_t	Final concentration of lead
K_f	Indicator of adsorption capacity
q_e	Quantity of adsorbate adsorbed on membrane, mg/g
q_m	Maximum adsorption capacity, mg/g
R^2	Linear regression value
S_q	Root-mean-square height, nm
w_w	Weight of wet membrane, g
w_d	Weight of dried membrane, g
$1/n$	Intensity of adsorption

Greek Symbols

ε	Porosity, %
ρ_p	Polyethersulfone density, g/cm^3
ρ_w	Water density, g/cm^3

Abbreviations

AFM	Atomic force microscopy
DOE	Design of experiment
GO	Graphene oxide
GPN	Graphene oxide polymer nanocomposite
NIPS	Non-solvent induced phase separation
PES	Polyethersulfone
PVP	Polyvinylpyrrolidone
SEM	Scanning electron microscopy

References

1. Arbabi, M.; Hemati, S.; and Amiri, M. (2015). Removal of lead ions from industrial wastewater, a review of removal methods. *International Journal of Epidemiologic Research,* 2(2), 105-109.

2. Ali, H.; Khan, E.; and Ilahi, I. (2019). Environmental chemistry and ecotoxicology of hazardous heavy metals, environmental persistence, toxicity, and bioaccumulation. *Journal of Chemistry*, 2019, Article ID 6730305, 1-14.

3. Vu, H.H.T.; Gu, S.; Thriveni, T.; Khan, M.D.; Tuan, L.Q.; and Ahn, J.W. (2019). Sustainable treatment for sulfate and lead removal from battery wastewater. *Sustainability,* 11(3497), 1-8.

4. Department of Environment. (2015). Malaysia Environmental Quality Report ofEnvironment Knowledge Management Centre, Malaysia. Retrieved September 18, 2018, from https://enviro2.doe.gov.my/ekmc/wp-content/uploads/2016/09/1-EQR-2015-Pendahuluan-1.pdf

5. Khulbe, K.C.; and Matsuura, T. (2018). Removal of heavy metals and pollutants by membrane adsorption techniques. *Applied Water Science,* 8(1), 1-30.

6. Madhura, L.; Kanchi, S.; Sabela, M.I.; Singh, S.; Bisetty, K.; and Inamuddin. (2018). Membrane technology for water purification. *Environmental Chemistry Letters,* 16(2), 343-365.

7. Sun, H.; Tang, B.; and Wu, P. (2017). Development of hybrid ultrafiltration membranes with improved water separation properties using modified super-hydrophilic metal-organic framework nanoparticles. *ACS Applied Materials and Interfaces,* 9(25), 21473-21484.

8. Qu, X.; Alvarez, P.J.J.; and Li, Q. (2013). Applications of nanotechnology in water and wastewater treatment. *Water Research*, 47(12), 3931-3946.

9. Bora, T.; and Dutta, J. (2014). Application of nanotechnology in wastewater treatment- a review. *Journal of Nanoscience and Nanotechnology,* 14 (1), 613-626.

10. Dave, P.N.; and Chopda, L.V. (2014). Application of iron oxide nanomaterials for the removal of heavy metals. *Journal of Nanotechnology,* 2014, 1-14.

11. Mohd, A.U.; Imran, K.; Bhat, A.H.; Pillai, R.S.; Mohamad-Hafiz, M.K.; Mohammad, O.. (2017). Current trend in the application of nanoparticles for wastewater treatment and purification, a review. *Current Organic Synthesis,* 14, 1-21.

12. Paul, D.R. (2012). Creating new types of carbon-based membranes. *Science*, 335(6067), 413-414.

13. Vo, T.S.; Hossain, M.M.; and Jenog, H.M. (2020). Heavy metal removal applications using adsorptive membranes. *Nano Convergence*, 7(36), 1-26.

14. Ma, J.; Ping, D.; and Dong, X. (2017). Recent developments of graphene oxide-based membranes, a review. *Membranes,* 7(52), 1-29.

15. Huang, K.; Liu, G.; Lou, Y.; Dong, Z.; Shen, J.; and Jin, W. (2014). A graphene oxide membrane with highly selective molecular separation of aqueous organic solution. *Angewandte Chemie International Edition,* 53(27), 6929-6932.

16. Pan, G.; Wang, L.; Song, S.; Xu, Z.; Fu, D.; and Zhang, G. (2018). Preparation of modified graphene oxide nanomaterials for water and wastewater treatment. *IOP Conference Series, Earth and Environmental Science,* 170(032074), 1-6.

17. Liu, L.; Zhou, Y.; Xue, J.; and Wang, H. (2019). Enhanced anti-pressure ability through graphene oxide membrane by intercalating g-C_3N_4 nanosheets for water purification. *American Institute of Chemical Engineer Journal,* e16699, 1-13.

18. Mkhoyan, K.A.; Contryman, A.W.; Silcox, J.; Derek, A.; Eda, G.; Mattevi, C.; Miller, S. and Chhowalla, M. (2009). Atomic and electronic structure of graphene-oxide. *Nano Letters,* 9(3), 1058-1063.

19. Peng, W.; Li H.; Liu, Y.; and Song, S. (2017). A review on heavy metal ions adsorption from water by graphene oxide and its composites. *Journal of Molecular Liquids*, 230, 496-504.

20. Zhao, X.; Su, Y.; Liu, Y.; Li, Y.; and Jiang, Z. (2016). Free-standing graphene oxide-palygorskite nanohybrid membrane for oil/water separation. *ACS Applied Materials and Interfaces,* 8(12), 8247-8256.

21. Tang, Y. P.; Paul, D.R.; and Chung, T.S. (2014). Free-standing graphene oxide thin films assembled by a pressurized ultrafiltration method for dehydration of ethanol. *Journal of Membrane Science,* 458, 199-208.

22. Jia, Z.; Wang, Y.; Shi, W.; and Wang, J. (2016). Diamines cross-linked graphene oxide free-standing membranes for ion dialysis separation. *Journal of Membrane Science,* 520,139-144.

23. Liu, Y. (2017). Application of graphene oxide in water treatment. *IOP Conference Series, Earth and Environmental Science,* 94(012060), 1-6.

24. Wang, Z.; Wu, A.; Colombi Ciacchi, L.; and Wei, G. (2018). Recent advances in nanoporous membranes for water purification. *Nanomaterials,* 8(2), 1-19.

25. Luque-alled, J.M.; Abdel-karim, A.; Alberto, M.; Leaper, S.; Perez-page, M.; Huang, K.; Gorgojo, P. (2020). Polyethersulfone membranes, from ultrafiltration to nanofiltration via the incorporation of APTS functionalized-graphene oxide. *Separation and Purification Technology,* 230(115836), 1-12.

26. Jiang L.Y. (2016). *Encyclopedia of Membranes* (1st ed.). Switzerland: Springer-Verlag Berlin Heidelberg.

27. Loeb, S.; and Sourirajan, S. (1963). Water demineralization by means of an osmotic membrane. *Saline Water Conversion-II. Advances in Chemistry Series*; American Chemical Society, Washington, DC, USA, 28,117-132.

28. Baig, M.I.; Durmaz, E.N.; Willott, J.D.; and Vos, W.M. (2019). Sustainable membrane production through polyelectrolyte complexation induced aqueous phase separation. *Advanced Functional Materials,* 1907344, 1-10.

29. Hasbullah, H.; Sabri, N.S.M.; Said, N.; Rosid, S.M.; Roslan, M.I.; Ismail, A.F.; Jye, L.W.; and Yusof, N. (2018). *Nanotechnology in Water and Wastewater Treatment: Theory and Applications* (1st ed.). Amsterdam: Elsevier Inc.

30. Ihsanullah, A.A.; Al-Amer, A.M.; Laoui, T.; Al-Marri, M.J.; Nasser, M. S.; Khraisheh, M.; and Atieh, M. A. (2016). *Separation and Purification Technology* (1st ed.). Amsterdam: Elsevier Inc.

31. Cui, Z.F.; Jiang, Y.; and Field, R.W. (2010). *Membrane Technology* (Reprint ed.). Oxford: Elsevier Ltd.

32. Fahrina, A.; Maimun, T.; Syarifah, H.;Rosnelly, C.M.; Mirna, R.L.; Intan, B.;, Rahmat, S.;, Ahmad, G.; and Arahman, N. (2018). The morphology and filtration performances of poly(ether sulfone) membrane fabricated from different polymer solution. *MATEC Web Conferences,* 3rd Annual Applied Science and Engineering Conference , 197 (2018) 09001, 1-4.

33. Wang, X.; Feng, M.; Liu, Y.; Deng, H.; Lu, J. (2019). Fabrication of graphene oxide blended polyethersulfone membranes via phase inversion assisted by electric field for improved separation and antifouling performance. *Journal of Membrane Science,* 577, 41-50.

34. Junaidi, N.F.D.; Othman, N.H.; Shahruddin, M.Z.; Alias, N.H.; Lau, W. J.; and Ismail, A.F. (2019). Effect of graphene oxide (GO) and polyvinylpyrollidone (PVP) additives on the hydrophilicity of composite polyethersulfone (PES) membrane. *Malaysian Journal of Fundamental and Applied Sciences*, 15(3), 361-366.

35. Abdel-Karim, A.; Gad-Allah, T.A.; El-Kalliny, A.S.; Ahmed, S.I.A.; Souaya, E.R.; Badawy, M.I.; and Ulbricht, M. (2017). Fabrication of modified polyethersulfone membranes for wastewater treatment by submerged membrane bioreactor. *Separation and Purification Technology,* 175, 36-46.

36. Nik Abdul Ghani, N.R.; Jami, M.S.; and Ku Abdullah, K.M.Z. (2019). Adsorption studies of graphene oxide for lead removal from synthetic wastewater. *Biological and Natural Resources Engineering Journal,* 2(2), 21-36.

37. Maximous, N.N.; Nakhla, G.F.; and Wan, W.K. (2010). Removal of heavy metals from wastewater by adsorption and membrane processes, a comparative study. *International Journal of Environmental and Ecological Engineering,* 4(4), 125-130.

38. Shahrin, S.; Lau, W.J.; Goh, P.S.; Ismail, A.F.; and Jaafar, J. (2019). Adsorptive mixed matrix membrane incorporating graphene oxide-manganese ferrite (GMF) hybrid nanomaterial for efficient As(V) ions removal. *Composites Part B Engineering,* 175(107150), 1-10.

39. Al-Ghouti, M.A.; Da'ana, D.; Abu-Dieyeh, M.; and Khraisheh, M. (2019). Adsorptive removal of mercury from water by adsorbents derived from date pits. *Scientific Reports*, 9(1), 1-15.

40. Amosa, M.K.; Jami, M.S.; and Alkhatib, M.F.R. (2016). Electrostatic Biosorption of COD, Mn and H_2S on EFB-based activated carbon produced throughsteam pyrolysis, an analysis based on surface chemistry, equilibria and kinetics. *Waste and Biomass Valorization,* 7(1), 109-124.

41. Freundlich, H.M. (1906). Over the adsorption in solution. *Journal of Physical Chemistry A*, 57, 385-470.

42. Tan, C.H.; Moo, Y.C.; Mat Jafri, M.Z.; and Lim, H.S. (2014). UV spectroscopy determination of aqueous lead and copper ions in water. *SPIE Photonics Europe Conference, Proceedings of SPIE- The International Society for Optical Engineering.* Wales, United States of America, 1-6.

43. Bayuo, J.; Abukari, M.A.; and Pelig-Ba, K.B. (2020). Desorption of chromium (VI) and lead (II) ions and regeneration of the exhausted adsorbent. *Applied Water Science*, 10(7), 1-6.

44. Amid, M.; Nabian, N.; and Delavar, M.(2020). Fabrication of polycarbonate ultrafiltration mixed matrix membranes including modified halloysite nanotubes and graphene oxide nanosheets for olive oil/water emulsion separation. *Separation and Purification Technology,* 11732, 1-49.

45. Akbari, M.; Shariaty-Niassar, M.; Matsuura, T.; and Ismail A.F. (2018) Janus graphene oxide nanosheet: A promising additive for enhancement of polymeric membranes performance prepared via phase inversion. *Journal of Colloid and Interface Science*, 527,10-24.

46. Kinloch, I.A.; Suhr, J.; Lou, J.; Young, R.J.; and Ajayan, P.M. (2018). Composites with carbon nanotubes and graphene, an outlook. *Science*, 362(6414), 547-553.

47. Sun, B.; Kong, F.; Zhang, M.; Wang, W.; Birat-Singh, K.C.; Tjong, J.; and Sain, M. (2020). Percolation model for renewable-carbon doped functional composites in packaging application, a brief review. *Coatings,* 10(2), 193-198.

48. Mahmoudi, E.; Ang, W.L.; Ng, C.Y.; Yong N.L.; Mohammad, A.W.; and Benamor, A. (2019). Distinguishing characteristics and usability of graphene oxide based on different sources of graphite feedstock. *Journal of Colloid and Interface Science,* 542, 429-440.

49. Kang, Y.; Obaid, M.; Jang, J.H.; Moon-ho, K.; and In, S. (2019). Novel sulfonated graphene oxide incorporated polysulfone nanocomposite

membranes for enhanced-performance in ultrafiltration process. *Chemosphere,* 207, 581-589.

50. Zinadini, S.; Zinatizadeh, A.A.; Rahimi, M.; Vatanpour, V.; and Zangeneh, H. (2014). Preparation of a novel antifouling mixed matrix PES membrane by embedding graphene oxide nanoplates. *Journal of Membrane Science,* 453, 292-301.

51. Bhatti, H.T.; Ahmad, N.M.; Khan Niazi, M.B.; Ur-Rehman A.M.A.; Ahmad, N.; Anwar, M.N.; and Khan, A.U. (2018). Graphene oxide-PES-based mixed matrix membranes for controllable antibacterial activity against *Salmonella typhi* and water treatment. *International Journal of Polymer Science,* 2018,1-12.

52. Gholami, N.; and Mahdavi, H. (2018). Nanofiltration composite membranes of polyethersulfone and graphene oxide and sulfonated graphene oxide. *Advances in Polymer Technology,* 37(8), 3529-3541.

53. Najjar, A.; Sabri, S.; Al-Gaashani, R.; Atieh, M.A.; and Kochkodan, V. (2019). Antibiofouling performance by polyethersulfone membranes cast with oxidised multiwalled carbon nanotubes and arabic gum. *Membranes,* 9(2), 1-26.

54. Kumar, M.; Chung, J.S.; and Hur, S.H. (2019). Graphene composites for lead ions removal from aqueous solutions. *Applied Sciences,* 9(14), 2925.

55. Alghamdi, A.A.; Al-Odayni, A.B.; Saeed, W.S.; Al-Kahtani, A.; Alharthi, F.A.; and Aouak, T. (2019). Efficient adsorption of lead (II) from aqueous phase solutions using polypyrrole-based activated carbon. *Materials*, 12(12), 1-16.

56. Khan, T.; Binti Abd Manan, T.S.; Isa, M.H.; Ghanim, A.; Beddu, S.; Jusoh, H.; Iqbal, M.S.; Ayele, G.T.; and Jami, M.S. (2020). Modeling of Cu(II) adsorptionfrom an aqueous solution using an artificial neural network (ANN). *Molecules*, 25(14), 1-15.

57. Mai, Z. (2013). *Membrane processes for water and wastewater treatment: Study and modeling of interactions between membrane and organic matter.* PhD dissertation. Ecole Centrale Paris.

58. Zhang, X.; Liu, Y.; Sun, C.; Ji, H.; Zhao, W.; Sun, S.; and Zhao, C. (2015). Graphene oxide-based polymeric membranes for broad water pollutant removal. *RSC Advances,* 5(122), 100651-100662.

59. Zheng, G.; Ye, H.; Zhang, Y.; Li, H.; Lin, L.; and Ding, X. (2014). Removal of heavy metal in drinking water resource with cation-exchange resins (Type 110-H) mixed PES membrane adsorbents. *Journal of Hazardous, Toxic and Radioactive Waste,* 19(2), 1-6.

60. Mahmoudi, E.; Ng, L.Y.; Ang, W.L.; Chung, Y.T.; Rohani, R.; and Mohammad, A.W. (2019). Enhancing morphology and separation performance of polyamide 6,6 membranes by minimal incorporation of silver decorated graphene oxide nanoparticles. *Scientific Reports*, 9(1), 1-16.

61. Mukherjee, R.; Bhunia, P.; and De, S. (2016). Impact of graphene oxide on removal of heavy metals using mixed matrix membrane. *Chemical Engineering Journal*, 292, 284-297.